Engineering Conferences International
ECI Digital Archives

Summer 6-25-2014

Studies on permeability properties and particle capture efficiencies of porous SiC ceramics processed by oxide bonding technique

Atanu Dey
Central Glass and Ceramic Research Institute

Nijhuma Kayal
Central Glass and Ceramic Research Institute

Omprakash Chakrabarti
Central Glass and Ceramic Research Institute

Rafael Caldato
University of Ribeirão Preto

Caio Andre
University of Ribeirão Preto

See next page for additional authors

Follow this and additional works at: http://dc.engconfintl.org/porous_media_V

🔴 Part of the Materials Science and Engineering Commons

Recommended Citation

Authors

Atanu Dey, Nijhuma Kayal, Omprakash Chakrabarti, Rafael Caldato, Caio Andre, Murilo Innocentini, and Vadila Guerra

STUDIES ON PERMEABILITY PROPERTIES AND PARTICLE CAPTURE EFFICIENCIES OF POROUS SiC CERAMICS PROCESSED BY OXIDE BONDING TECHNIQUE

Atanu Dey,* Nijhuma Kayal, and Omprakash Chakrabarti
Central Glass and Ceramic Research Institute, CSIR, Kolkata-700 032, West Bengal, India

Rafael F. Caldato, Caio M. André, and Murilo D.M. Innocentini,
Course of Chemical Engineering, University of Ribeirão Preto (UNAERP), 14096-900 Ribeirão Preto, SP, Brazil
Vadila G. Guerra
Department of Chemical Engineering, Federal University of São Carlos (UFSCar),13565-905 São Carlos, SP, Brazil
*E-mail of corresponding author: atanudey2000@gmail.com

ABSTRACT

Porous SiC ceramics bonded with mullite (MBS of fractional porosity (ε) of 0.29-0.56, average pore size (d_{pore}) of 5-11 μm, flexural strength (σ) of 9-34 MPa and elastic modulus (E) of 7-28GPa) and cordierite (CBS with ε of 0.33-0.72, d_{pore} of 6-50 μm, σ of 5-54 MPa and E of 6-42 GPa) were prepared by heating in air at 1350-1500°C compacts of desired amounts of SiC, Al_2O_3 and MgO powders and petroleum coke dust as the pore former. Air permeation behavior of well-characterized samples was studied with fluid superficial velocity (v_s) from 0.08 to 1.0 m s^{-1}and at RT to 750°C. The Darcian (k_1) and non-Darcian (k_2) permeability coefficients were evaluated by fitting the Forchheimer's equation to experimental pressure drop-superficial velocity data. Porosity dependence of permeability coefficients was explained in terms of structural characteristics. Changes in pressure drop experienced by the porous ceramics at high temperatures were explained by temperature dependence of permeability coefficients and variation of fluid properties. Collection efficiency (η) of filter ceramics operating on removal of solid NaCl nanoaerosol particles (of 7-300 nm size) was determined from particle counts before and after filtration at v_s = 0.05-0.10 m s^{-1}. Experimental results showed variation of η from 96.7 to 99.9% for change of ε from 0.56 to 0.68. The size-selective fractional collection efficiency at different porosity levels was derived using the well-known single-collector efficiency model considering some boundary conditions and the model data were validated with experimental results. The test results were used to examine the applicability of the filter ceramics in nanoparticle filtration processes.

INTRODUCTION

Industries that have dangerous processes with off-gases laden with fine particles have become a vital concern for public health and environmental safety. Increasing particle pollution in air has led to increasing regulations in order to control and limit the atmospheric particulate pollutant. Many important industrial processes, such as coal/biomass combustion/gasification for power generation, thermal remediation of contaminated soils, incineration of biomedical and industrial wastes, metal smelting, manufacturing of cement, carbon black, glass, etc. emit through off-gases particulate matters (PM) into atmospheric environment. Fine particle control is indeed a concern for these thermal industries for abatement of air pollution. In 1970s, it became first recognized that fine particles from industrial processes and automobiles have a significantly more negative effect on public health and environment than the relatively larger particles of windblown dust. Particles with aerodynamic diameter less than 10 μm (referred to as PM 10) were targeted for removal [1]. For stringent environmental control, acceptable limits of airborne particles finer than 2.5 μm (PM 2.5) were later regulated [1]. Pressure has been building up to tighten the standard to PM 0.1 (particles finer than 0.1 μm) [2]. With particle in this ultrafine range, impacts on human health are more pronounced due to an increased relative toxic concentration as well as ready respirability. These regulations force the industrial processes to have certain control over the fine particle emissions. Control of fine particles in waste industrial gases at high temperatures and severe conditions can be very effectively achieved by ceramic filters. Porous SiC ceramics are promising filtering media as they have low bulk density, excellent mechanical strength and chemical stability, high thermal conductivity, superb thermal shock resistance and they can withstand high temperatures and hostile atmospheres. Processing routes are found to synthesize porous SiC ceramics without sacrificing these special properties. Oxide bonding is indeed a very useful technique to prepare the materials [3-7]. The technique is simple and inexpensive because it does not require any sophisticated equipment, delicate instrumentation and attainment of very high temperatures. Mullite and cordierite serve as very effective oxide bonds as they have very good thermal and chemical stability, low or matching thermal expansion coefficient with SiC and

ability to be processed at low temperatures as bonds for SiC. There is another issue. In industrial indoor environments where clean air is needed to avoid contamination from fine hazardous dusts and polluting action on workers and products, high efficiency particulate air (HEPA) filters (to control PM <0.1 with 99.99% efficiency or more) are recommended. Use of ceramic HEPA filters may be advantageous, as they can withstand severely aggressive environments and possess very high strength compared to the conventional HEPA filter materials (polymers/glass fibers) although they may not need to face the same high temperature levels of off-gas cleaning processes. Conventional materials are flexible and can be fold-shaped producing a large area in a small volume (cartridge), saving a lot of space and reducing pressure drop significantly due to small superficial fluid velocities for a given flow rate. These advantages are possible to be achieved for SiC ceramic HEPA filters by suitable modification of the design of the filter ceramics and also the design of the entire filter device [8]. In this backdrop the focus of the present paper is to evaluate performance of mullite and cordierite bonded SiC ceramics for their possible applications as filtering media for industrial off-gas cleaning and particle control in industrial indoor environment. Processing parameters and gas permeation behavior of the ceramics were investigated. Experimental data of solid nanoaerosol filtration were acquired and compared to the existing models in order to determine best parameters for the optimized filter composition.
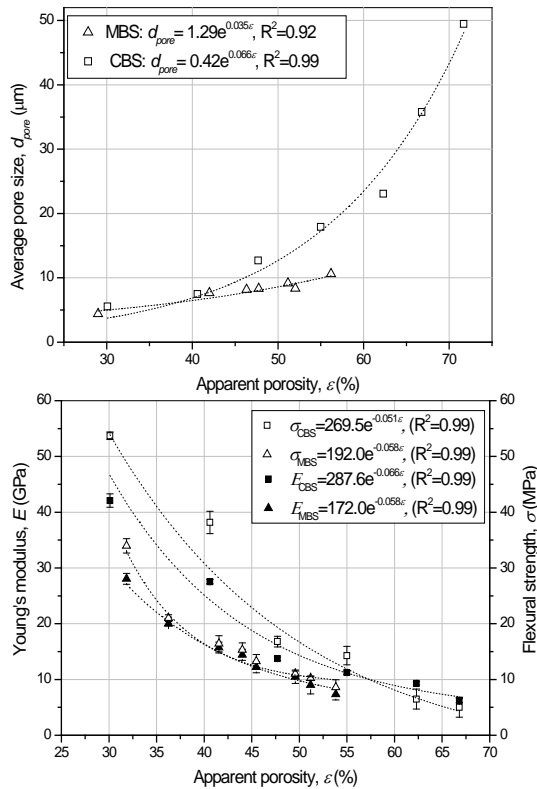

Figure1: Porosity dependence of d_{pore} (top) and mechanical properties (bottom) of MBS and CBS.

EXPERIMENTAL

Powders of SiC (α-SiC; purity 98.2% (w/w); d_{50} = 22.5 μm; Grindwell Norton Ltd., Mumbai, India), Al_2O_3 (α-Al_2O_3; Purity >98% (w/w); d_{50} = 6.5 μm; Indian Aluminium Co. Ltd., Howrah, India), MgO (Purity >97% (w/w); d_{50} = 4.5 μm; Mark Specialties India Pvt. Ltd., Mumbai, India) and petroleum coke (ash content, 0.68% (w/w); d_{50} = 11.4 μm; Assam Carbon Products Ltd., Kolkata, India) as the pore former were used. For mullite bonding the weight ratio of Al_2O_3 to (Al_2O_3+SiC) was maintained at 0.2. For Cordierite bonding weight ratios of (Al_2O_3+MgO) to (Al_2O_3+MgO+SiC) of 0.2 and Al_2O_3 to MgO of 2.5 were used. The fractional volume of pore former varied between 0.15 and 0.76. The powders were suitably mixed in a liquid medium, dried powders were pressed in the form of bars (47×20×13 mm³) and discs (40 mm diameter × 10 mm thickness), well dried pressed bodies were fired at 1100°C for 4h in air for burning of pore former followed by further heat treatment at higher temperatures for 4h in air for oxide bonding. For mullite and cordierite bonding the heat treatment temperatures were selected as 1350 and 1500°C, respectively, based on the results of thermal analysis of starting powders. Apparent porosity (ε) of oxide bonded SiC samples was measured by water immersion method. XRD analysis was done by using a PW 1710 (Philips, Eindhoven, The Netherlands) diffractometer with Cu K_α radiation of the wavelength of 1.5406Å. The weight percentages of crystalline phases were estimated by X-ray diffraction line profile analysis following Rietveld refinement method and using X'Pert High Score Plus software (version 3.0e, PANalyticl B.V.); recorded variations of different assessment indices were: R_{WP} from 11.9 to 19.9, R_P from 10.2 to 17.7, R_{exp} from 12 to 16 and GOF from 1.0 to 1.7, indicating acceptable fitting quality. Microstructural examination was done by scanning electron microscopy (Model SE 440, Leo-Cambridge, Cambridge, UK) The average pore size (d_{Pore}) and pore size distribution were evaluated by Hg-intrusion porosimetry method (Poremaster, Quantachrome Instruments Inc., Florida, USA). Room temperature 3 pt. flexural strength was determined in an UTM machine (Model 1123, Instron Corporation, Norwood, MA, USA; sample dimensions: 45×4.5×3.5 mm³; span: 40 mm; loading rate: 0.5 mm min⁻¹). Young's modulus was determined from the slope of the load deflection curves using standard software (Instron Bluehill-2, Bucks, UK). The gas permeation behavior was studied by conducting airflow test in a laboratory set up following the procedure described in ref. [9]. The disc sample (of 1.54 cm² circular flow area, A_{flow}) was suitably placed in a sample holder which was then fitted in a metallic cylinder in perfectly sealed condition. Air was passed through the sample and v_S (= Q/A_{flow}) was changed (0.08-1.0 m s⁻¹) by varying the volumetric flow rate (Q). The whole system was put in an electric furnace and the sample temperature was varied from room temperature to 750°C. The pressure drop (inlet pressure,

P_i and outlet pressure, P_o) was measured across the sample and plotted as pressure drop relative to unit sample thickness versus v_S as function of temperature. The filtration behavior was studied by conducting the dust collection efficiency test at room temperature with v_S ranging from 0.05-0.10 m s^{-1} using NaCl nanoparticles (of density 2165 kg m^{-3} and size range of 7 to 300 nm) following procedures of ref. [9]. NaCl nanoparticles were generated in an aerosol generator (Model 3079, TSI Incorporated, USA), dispersed in clean air and the aerosol after neutralization of electric charges, was finally passed through the sample. The size distribution of particles of the aerosol stream was determined at the inlet and outlet by a Scanning Mobility Particle Sizer, SMPS (Model 3936; TSI Incorporated, USA), essentially consisting of an Electrostatic Classifier (Kyrpton-85 Neutralizer, Model 3012; TSI Incorporated, USA) coupled to a long Differential Mobility Analyzer, DMA (Model 3085; TSI Incorporated, USA) and an Ultrafine Condensation Particle Counter, UCPC (Model 3776; TSI Incorporated, USA).
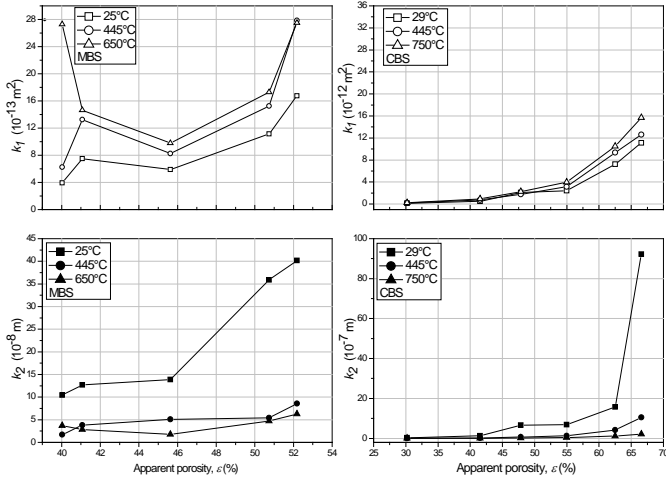

Figure 2: Porosity dependence of k_1 and k_2 as function of temperature for MBS (L) and CBS (R).

RESULTS & DISCUSSION

After oxide bonding the samples exhibited no significant dimensional or linear shrinkage; shape distortion or surface cracks were not evident. For MBS and CBS samples, the recorded variation of ε was from 0.29 to 0.56 and 0.33 to 0.72, respectively; XRD analysis detected in these samples α-SiC (hexagonal, space group P63mc, $a=b=3.0810$Å, $c=15.12$Å, $\alpha=\beta=90°$ and $\gamma=120°$) and cristobalite (low, tetragonal, space group P41212, $a=b=4.9823$Å, $c=6.9638$Å, $\alpha=\beta=\gamma=90°$) as the common crystalline phases; MBS ceramics contained mullite (orthorhombic, space group Pbam, $a=7.5456$Å, $b=7.6898$Å,$c=2.8842$Å, $\alpha=\beta=\gamma=90°$) and cordierite (orthorhombic, space group Cccm, $a=17.0470$Å, $b=9.7315$Å, $c=9.3463$Å, $\alpha=\beta=\gamma=90°$) was present in CBS samples. The variations of amount of crystalline phases in the MBS samples were from 35 to 45% w/w for SiC, 30 to 39% w/w for cristobalite and 19 to 26%

w/w for mullite. The CBS samples had variations in the amount of SiC, cristobalite and cordierite from 51 to 56, 24 to 27 and 21 to 23% w/w. Microstructural examination revealed formation of oxide bond in the bridging necks between contacting SiC particles, presence of crystalline phases such as cristobalite and mullite/cristobalite in the bonds, coating of SiC particles with a viscous (glassy) phase and open-cell pore morphology. Figure 1 shows the porosity effect on pore size and mechanical properties of the porous ceramics. The experimental d_{pore} and ε data were fitted to an exponential relation with a fairly good fitting quality. The pore size relative to porosity was higher in CBS than MBS samples. In both MBS and CBS samples presence of viscous (liquid) phases were evident in the microstructures. It is likely that the glasses in MBS sample had aluminosilicate compositions and in CBS samples they had also aluminosilicate compositions with network modifier cation Mg^{+2}. Oxygen occupied either bridging (BO) or non-bridging sites (NBO) in these glassy materials. The bridging oxygen (BO) species connected the AlO$_4$ and SiO$_4$ tetrahedra, thereby providing strong bonds between the structural units of aluminosilicate network and increasing viscosity whereas the non-bridging oxygen (NBO) species provided a relatively weak link between the tetrahedral cations (Si or Al) and the network modifier cation (that was not integral part of the tetrahedral network) decreasing viscosity of the corresponding liquid [10]. It can be understood from this fact that in CBS samples the lowly viscous glass flowed into some small pores and filled them up so that only larger pores were left and the average diameter of the pores increased. In the MBS samples the high viscosity might have restricted the flow of the glass to fill the small pores decreasing the pore size. With the increase in porosity possibility of interconnection between void spaces also increased raising the pore size. The experimental mechanical property ~ flexural strength (σ) and Young's modulus (E) ~ and ε data were also fitted very well to exponential relations indicating that the pores were extremely interconnected and the materials' mechanical behavior was like that of cellular solids. The higher strength and elastic modulus of CBS samples than MBS samples might be related to the higher SiC content of the former than the latter.

The experimental pressure drop (normalized) and face velocity data for airflow under ambient conditions ($T_o \approx$ 29°C; P_o= 95.06 k Pa; air density, ρ = 1.1 kg m^{-3}; air viscosity μ = 1.88×10^{-5} Pa s) were fitted very well to the Forchheimer's model [11]:

$$\frac{P_i^2 - P_o^2}{2P_o L} = \frac{\mu v_s}{k_1} + \frac{\rho v_s^2}{k_2} \tag{1}$$

where k_1 and k_2 are, respectively, the Darcian and the non-Darcian permeability coefficients and L is the

sample thickness. The permeability coefficients k_1 and k_2 were determined from the constants of the linear and quadratic terms of Eq. (1) and fluid properties (μ and ρ). In a similar way k_1 and k_2 at higher temperatures were determined from the fitting equations of experimental normalized pressure drop and v_s data (recorded at those temperatures) to the Forchheimer's model and the fluid properties (at conditions of those temperatures). Figure 2 shows the porosity dependence of k_1 and k_2 as a function of temperature for the MBS and CBS ceramics. Permeability coefficients increased with porosity for the two types of materials. The variation of room temperature k_1 was from 7.6×10^{-13} to 1.6×10^{-12} m^2 and 21.0×10^{-13} to 11.1×10^{-12} m^2, respectively for materials with mullite and cordierite bonding, at $\varepsilon >47.5\%$, indicating that the ranges of k_1 were within the limits of permeability coefficients typical for hot aerosol filters ($\approx10^{-13}$ to 10^{-12} m^2) [12]. At $\varepsilon >47.5\%$, CBS samples were found to exhibit higher k_1 than MBS ceramics. At room temperature k_2 varied in the ranges of 1.3×10^{-9} to 2.7×10^{-9} m and 6.6×10^{-7} to 9.2×10^{-6} m, respectively, for the materials with mullite and cordierite bonds at $\varepsilon >47.5\%$. These ranges were also well within the typical limits of k_2 for hot aerosol filters [12]. The porosity dependence of k_1 and k_2 for the two ceramic materials can be examined by some established empirical relations, for example, the famous Ergun like equations, according to which the permeability coefficients are expressed as: $k_1 = (2.25\varepsilon d_{pore}^2)/150$ and $k_2 = (1.5\varepsilon^2 d_{pore})/1.75$ [13]. The empirical equations are derived on the basis of the assumptions that the porous media are constituted of loose spherical particles. These equations have been tested and validated for a varieties of porous media ~ unconsolidated and also consolidated ~ and only in case of consolidated porous media (partially sintered porous ceramics) the testing and validation have been done on condition that the size distribution of raw ceramic powders is representative in the consolidated product. Figure 3 represents the plots of experimental permeability coefficients versus the permeability coefficients predicted by Ergun like equations. One definite conclusion that can be drawn from the results is that while Ergun equation works fine for k_1 it is not reliable for k_2. This point is well documented in literature, as many empirical relations have been suggested to predict k_2 based on the values of k_1 obtained from Ergun equation [14,15]. One viable approach for prediction of k_2 from ε and d_{pore} may be based on the relationship between k_1 and k_2 derived from a large experimental data set and presented in the permeability map by Innocentini et al. [13]: $k_2 = \exp(-1.71588/k_1^{0.08093})$. Substitution of Ergun equation for k_1 thus gives: $k_2 = \exp\{-2.41044/(\varepsilon^{0.08093} d_{pore}^{0.16186})\}$. Following this approach k_2 was thus estimated from experimental ε and d_{pore} data and were plotted against experimental k_1 in Figure 3. The expression for k_2 derived on the basis of permeability map displayed a satisfactory and consistent predictability of the non-Darcian permeability in the entire range of experimental data related to the two porous SiC ceramic materials. At high temperatures the general trend was that both k_1 and k_2 also increased with porosity (Figure 2).
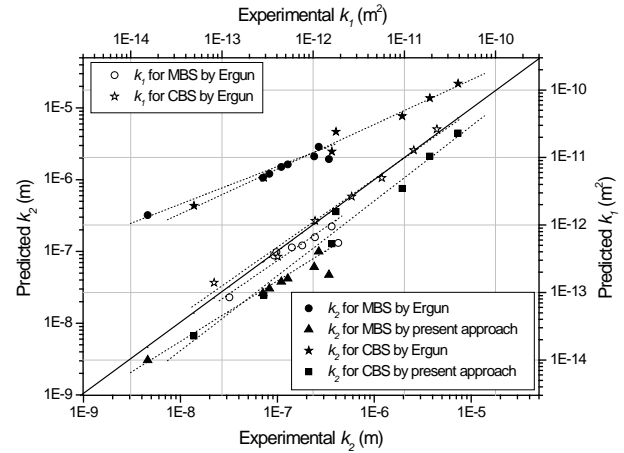

Figure 3: Comparison of prediction by Ergun equation and the approach proposed in the present work and experimental measurement of k_1 and k_2.

For MBS samples steady but small increase of k_1 with temperature was obtained except one with $\varepsilon \approx40\%$; slight decrease in k_1 from 445 to 650°C was observed at $\varepsilon \approx52\%$. The material exhibited a decrease in k_2 with temperature at all porosities, except at $\varepsilon \approx40\%$. Similar trends were also observed for CBS samples ~ a slight increase of k_1 and a decrease of k_2 with an increase of temperature from RT to 750°C was observed. The fluid properties change with temperature (for increase of temperature from RT to 750°C, the predicted increase in μ and decrease of ρ of air are 131 and 70% respectively). The average increase of k_1 and decrease of k_2 for MBS and CBS samples were around 40% and 71% and 84% and 94%, respectively. The changes of fluid properties raised the pressure drop with temperature according to the Forchheimer's equation. However the increase in k_1 with temperature could be beneficial (for low pressure drop decreases the pump power requirement during aerosol filtration), but the increase of fluid viscosity with temperature surpassed this beneficial effect, and the net effect was increase in pressure drop with temperature. The pressure drop can be reduced by increasing the permeability coefficients with increase in porosity. For application in hot aerosol filtration, clean and virgin filtering elements exhibit pressure drop values in the range of 1000-5000 Pa at 300-1500°C with $v_S = 0.05$ m s^{-1}. The MBS samples with $\varepsilon \approx55\%$, exhibited pressure drop at RT and 650°C of 5621 and 12945 Pa with $v_S = 0.05$ m s^{-1}, while the corresponding pressure drop exhibited by the CBS ceramics in similar conditions were 2963 and 5628 Pa. The pressure drop for the CBS materials at the two temperatures decreased to 343 and 673 Pa at $\varepsilon \approx67\%$, indicating that the samples with $\varepsilon >55\%$ are good candidates to be used as hot aerosol filters.

Dust collection efficiency test was conducted for MBS samples at $\varepsilon \approx 56\%$ and CBS samples at three levels of porosity ($\varepsilon = 62, 67$ and 68%). Fractional collection efficiency (E_{frac}) at each particle size (i-th particle) was determined from the particle mass concentration (in µg m^{-3}) for the particle measured at inlet ($C_{inlet,i}$) and outlet ($C_{outlet, i}$):

$$E_{frac} = \frac{C_{inlet,i} - C_{outlet,i}}{C_{inlet,i}} \qquad (2)$$

and the overall filter efficiency ($E_{overall}$) was determined from the total mass concentration (in µg m^{-3}) measured at inlet ($C_{inlet} = \sum_{i=7\,nm}^{300\,nm} C_{inlet,i}$) and outlet ($C_{outlet} = \sum_{i=7\,nm}^{300\,nm} C_{outlet,i}$):

$$E_{overall} = \frac{C_{inlet} - C_{outlet}}{C_{inlet}} \qquad (3)$$

The fractional collection efficiency can be calculated by the single collector efficiency model derived for granular filters considering that the filtration process is time independent (a condition valid for the initial stage of filtration with no dust cake formed on the filter surface):

$$E_{frac} = 1 - exp\left[-\frac{aKL(1-\varepsilon)\eta_T}{d_c}\right] \qquad (4)$$

where a is a fitting constant (in the present work a was considered to be unity), K is a function of ε ($=[6/(1-\varepsilon)^{2/3}]^{1/3}$) [16], d_c represents the average collector diameter (considered in the present work to be equal to the Sauter diameter (d_{vs}) of the raw SiC powder used to prepare the filter samples and η_T is the total collection efficiency of a single collector ~ a combination of the individual contributions due to different collection mechanisms like Brownian diffusion (η_d), inertia (η_I), direct interception (η_{DI}), gravity (η_G) and electrophoresis (η_E):

$$\eta_T = 1 - (1-\eta_D)(1-\eta_{DI})(1-\eta_I)(1-\eta_G)(1-\eta_E) \qquad (5)$$

The single collector electrophoretic efficiency was not considered as the NaCl nanoparticles were charged neutralized before they entered the filter. These mechanisms of arresting dust particles by filter media are well documented in published literature [9]. The expressions for individual contributions due to different collection mechanisms, all of which are functions of d_{pi} (= nanoparticle dust size), are discussed in details in these reported literatures. The contribution of each mechanism to the total single-collector efficiency (η_T) in the size range of dust particles from 7 to 300 nm for the porous SiC samples was determined, following the procedure described in ref. [9]. Figure 4 represents typical contribution of different dust collection mechanisms to the single-collector efficiency for MBS ceramics with $\varepsilon \approx 56\%$. The fractional filter efficiency (E_{frac}) was estimated as a function of d_{pi} for the porous

SiC samples by eqs. (4) and (5) and using experimental conditions (mean free path of air at room temperature and atmosphere pressure: $\lambda = 7.56\times10^{-8}$ m; air viscosity $\mu = 1.86\times10^{-5}$ Pa s; face velocity of aerosol $v_s = 0.05$-0.1 m s^{-1}). Figure 4 represents the plot of E_{frac} versus d_{pi} for the samples. A comparison between the modelling (theoretical) and experimental curves shows satisfactory agreement between the proposed correlation of E_{frac} with d_{pi} and the experimental results. The small differences that still exist between modelled and experimental data may be due to the fact that predictions are made on the basis of granular filter medium where the experiments were done using consolidated porous media of sintered ceramics. From the results presented in Figure 4 it is also clear that diffusional mechanisms plays the most dominant role on capture of nanoparticles by the filtering media. The overall efficiency was also estimated using the following expressions:

$$E_{overall} = \sum_{i=7\,nm}^{300\,nm} w_i E_{frac} \qquad (6)$$
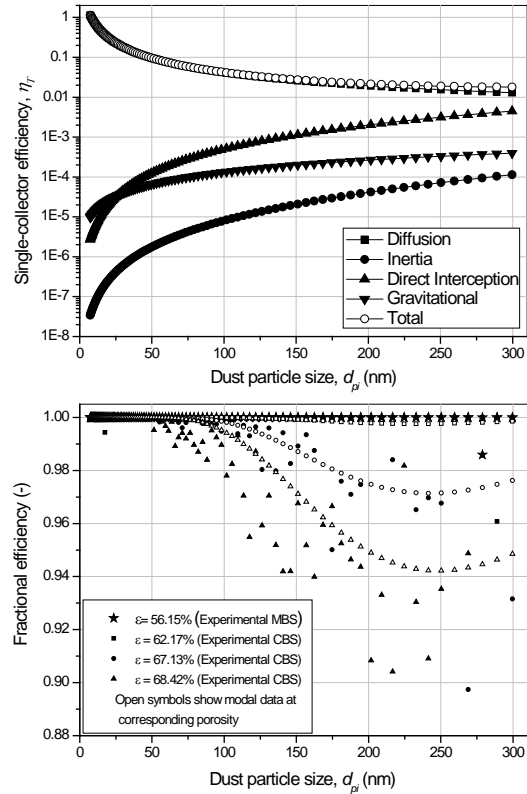
where, $w_i = C_{inlet,i}/C_{inlet}$ \qquad (7)

Figure 4: Different mechanisms' contributions to single-collector efficiency for MBS ceramics ($\varepsilon \sim 56\%$) (top); comparison between modeling and experimental curves of E_{frac} versus d_{pi} for MBS and CBS ceramics of porosity at different levels (bottom).

The estimated and experimental overall efficiencies agreed well for MBS ceramics (99.9%). For the CBS

ceramics these two efficiency parameters were 96.9 and 96.7, 98.5 and 98.6, 99.9 and 99.9, respectively at $\varepsilon =$ 68.4, 67.1 and 62.1%, indicating a decrease in dust collection mechanism with porosity. These figures show a very good agreement between the theoretical (model) and experimental $E_{overall}$ for the filter ceramics at different porosity level. The $E_{overall}$ results indicate strong application possibilities of porous SiC ceramics in nanoparticle filtration processes.

CONCLUSIONS

The present work successfully demonstrated synthesis of porous SiC ceramics bonded with mullite and cordierite by a simple and low temperature processing technique. The CBS samples exhibited higher pore size, strength and elastic modulus than MBS samples at comparable porosity levels because of certain advantages of constitutional characteristics (higher amount of crystalline SiC, lower viscosity of glassy phase, etc.). Permeability coefficients could increase several orders of magnitude depending on addition of sacrificial pore former indicating that it was possible to tailor these parameters according to the need of specific applications. The permeability coefficient of both the porous SiC with ε >48% was well within the range typical of hot aerosol filters. k_1, but not, k_2 fitted well to Ergun equation. From the relationship between k_1 and k_2 obtained by fitting large numbers of experimental permeability data in a permeability map, more reliable prediction for k_2 was possible by an equation proposed in the present work: $k_2 = \exp\{-2.41044/(\varepsilon^{0.08093} d_{pore}^{0.16186})\}$. Resistance to fluid flow increased with temperature because of increase of fluid viscosity with temperature. Resistance to fluid flow for CBS samples at ε >55%, remained in the range typical for hot aerosol filters, showing that the CBS ceramics are good candidates for application in hot aerosol filtration. For the MBS and CBS ceramics, size-selective fractional collection efficiency could be described by the single collector efficiency model derived for granular filters. 99.9% overall efficiency was obtained for the MBS and the CBS samples at respective porosity levels of 56 and 62%. The overall efficiency could also be reliably predicted by the single collector model. The decrease in $E_{overall}$ of CBS samples from 99.9% with increase in ε was likely related to the deleterious effects of porosity on diffusional mechanism. The overall efficiency data of the oxide bonded SiC ceramics indicate their strong application possibilities in nanoparticle filtration processes.

ACKNOWLEDGEMENT

REFERENCES

[1] Darcovich K, Jonasson KA, Capes CE (1997) Developments in the control of fine particulates air emissions. Adv. Powder Technol. 8:179-215.

[2] Howard CV (June 2009) Statement of Evidence: Particulate Emissions and Health. Proposed ringaskiddy waste-to-energy facility. Retrieved Aug. 4, 2013 at http://www.cawdrec.com/incineration/CVH.pdf.

[3] She JH, Deng ZY, Doni JD, Ohji T. (2002) Oxidation bonding of porous SiC ceramics. J. Mater. Sci. 37: 3615-3622.

[4] Chun YS, Kim YW (2005) Processing and mechanical properties of porous silica-bonded silicon carbide ceramics. Met. Mater. Int. 11: 351-355.

[5] She JH, Ohji T (2003) Fabrication and characterization of highly porous mullite ceramics. Mater. Chem. Phys. 80: 610-614.

[6] Bardhan N, Bhargave P (2008) In situ reaction sintering of porous mullite bonded SiC. Its mechanical behavior and high temperature application. Ceram. Eng. Sci. Proc. 29: 127-140.

[7] Dey A, Kayal N, Chakrabarti OP (2011) Preparation of mullite bonded porous SiC ceramics by an infiltration technique. J. Mater. Sci. 46: 5432-3438.

[8] Mitchell MA, Bergman W, Haslam J, Brown EP, Sawyer S, Beaulieu R, Althouse P, Mieke A (2012) Ceramic HEPA filter program. Presented at 32nd Nuclear air cleaning conference. International society for nuclear air treatment technologies. CO, USA, June 17-19. http://www.isnatt.org/Conferences/32/Tuesday/25%20LLNL-PROC-559284%20Ceramic%20HEPA%20Filter%20presentation%20for%20ISNATT.pdf

[9] Freitas NL, Goncalves JAS, Innocentini MDM, Coury JR (2006) Development of a double-layered ceramic filter for aerosol filtration at high-temperatures: The filter collection efficiency. J. Hazard. Mater. B 136: 747–756.

 [10] Sebbins JF, Xu Z (1997) NMR evidence for excess non-bridging oxygen in an aluminosilicate glass. Nature 390: 60-62.

[11] Scheidegger AE (1974) The physics of flow through porous media. In: Scheidegger AE. University of Toronto Press, Toronto.

[12] Purchas DB, Sutherland K (2002). Handbook of Filter Media; Elsevier Science and Technology Books: Amsterdam.

[13] Innocentini MDM, Sepulveda P, Ortega FS (2005) In Cellular Ceramics: Structure, Manufacturing, Properties and Applications; Scheffler, M, Colombo, P., Eds.; Wiley-VCH: Weinheim, Germany, pp.313-341.

[14] Meyer BA, Smith DW (1985) Flow through porous media: comparison of consolidated and unconsolidated material. Ind. Eng. Chem. Fundam. 24: 360-368.

[15] Narayanaswamy G, Sharma MM, Pope GA, (1999) Effect of heterogeneity on the non-Darcy flow coefficient. SPE Reservoir Eval. Eng. 2(3): 296-302.

[16] Yoshida H, Tien C (1985) A new correlation of the initial collection efficiency of granular aerosol filtration. AIChE J. 31: 1752-1754.